



ORIGINAL ARTICLE

Monitoring corrosion and corrosion control of low alloy ASTM A213 grade T22 boiler steel in HCl solutions

Mohammed A. Amin *, Gaber A.M. Mersal, Q. Mohsen

Materials and Corrosion Lab, Faculty of Science, Chemistry Department, Taif University, 888 Hawaiya, Saudi Arabia

Received 15 April 2010; accepted 21 June 2010

Available online 26 June 2010

KEYWORDS

Monitoring corrosion rates;
Low alloy steel;
Ser;
Tafel extrapolation method;
EFM;
XPS

Abstract Rates of corrosion of low alloy ASTM A213 grade T22 boiler steel were monitored in aerated stagnant 0.50 M HCl solutions at different temperatures (283–303 K) using Tafel extrapolation method and the non-destructive electrochemical frequency modulation (EFM) technique, complemented with XPS examinations. Serine (Ser) was introduced as a corrosion-safe inhibitor. Corrosion rates (in $\mu\text{m y}^{-1}$) obtained from these two methods was in good agreement. Tafel plots showed that Ser acted mainly as a cathodic-type inhibitor. The inhibition process was attributed to the formation of an adsorbed film on the metal surface that protects the metal against corrosive agents. XPS examinations of the electrode surface confirmed the existence of such adsorbed film. The inhibition efficiency increased with increase in Ser concentration, while it decreased with temperature, suggesting physical adsorption. Activation energies have been calculated in the absence and presence of various concentrations of Ser by measuring the temperature dependence of the corrosion rate obtained from the two methods employed. It was found that the activation energy in the presence of Ser is higher than that in bare HCl solution. The adsorptive behaviour of Ser followed Temkin-type isotherm. The standard free energy of adsorption was estimated to be -25 kJ mol^{-1} at 303 K. These results confirmed the occurrence of physical adsorption.

© 2010 King Saud University. Production and hosting by Elsevier B.V. All rights reserved.

* Corresponding author. Tel.: +44 1305 251066; fax: +44 1305 251908.

E-mail address: maaismail@yahoo.com (M.A. Amin).

1878-5352 © 2010 King Saud University. Production and hosting by Elsevier B.V. All rights reserved.

Peer review under responsibility of King Saud University.

doi:10.1016/j.arabjc.2010.06.040



Production and hosting by Elsevier

1. Introduction

Inhibitors are generally used to control metal dissolution (Behpour, 2009; Balaji and Upadhyaya, 2009; Sundararajan et al., 2009; Rao and Singhal, 2009; Okayasu et al., 2009). Most of the well-known acid inhibitors are organic compounds containing nitrogen, sulfur, and oxygen atoms. The strict environmental regulations and the increasing of ecological awareness have resulted in the use of substitute nontoxic compounds, acceptable from the environmental point of view “green inhibitors” (Lebrini et al., 2008; Oguzie et al., 2007).

In a continuation of our previous study (Amin et al., 2009a,b), the objective of the present work is to inhibit corrosion of low chromium alloy steel SA213-T22 in 0.50 M HCl solution. To achieve this goal, serine (Ser) is applied as a corrosion-safe inhibitor. Measurements were conducted using Tafel polarization and EFM techniques. Rates of corrosion measured by Tafel extrapolation method were compared with those recorded from the EFM technique. The aim is to confirm validation of corrosion rates measured by Tafel extrapolation method. The objective here also is to investigate the temperature dependence of the corrosion rate with the aim to obtain the apparent activation energies of the corrosion process of steel in 0.50 M HCl solutions in the absence and presence of different concentrations of Ser. It was also the purpose of the present work to test the experimental data with several adsorption isotherms at different temperatures, in order to determine the standard free energies of the adsorption process and gain more information on the mode of adsorption of the inhibitor on the electrode surface. XPS examinations of the electrode surface in presence of 10 mM Ser were also carried out.

2. Experimental

The working electrode employed in the present work was made of low alloy steel (ASTM A213 grade T22), this type of alloy is widely used as a super-heater pipe at steam power plants. The composition of the low alloy steel was determined using Energy Dispersive X-ray spectroscopy (EDX) and presented elsewhere (Amin et al., 2009b). Electrochemical measurements were carried out in a conventional electrochemical cell containing three compartments for working (with an exposed area of 1.0 cm²), a platinum foil (1.0 cm²) counter and reference electrodes. A Luggin–Haber capillary was also included in the design. The reference electrode was a saturated calomel electrode (SCE) used directly in contact with the working solution. The experiments were conducted in a 150 cm³ volume cell at 30 °C ± 2 using a temperature control water bath. The measurements were carried out in aerated non-stirred 0.5 M HCl solutions without and with various concentrations of serine (Ser), Fig. 1, as a safe corrosion inhibitor.

Polarization measurements were carried out starting from a cathodic potential of −0.60 V to an anodic potential of 0.0 V at a sweep rate of 0.50 mV s^{−1}. The linear Tafel segments of the cathodic curves and the calculated anodic Tafel lines were extrapolated to corrosion potential to obtain the corrosion current densities (j_{corr}) Amin et al., 2009a,b. The inhibition efficiency, $I_{\text{Tafel}}(\%)$, was evaluated from the measured j_{corr} values using the relationship:

$$I_{\text{Tafel}}(\%) = 100 \times [(j_{\text{Ocorr}} - j_{\text{corr}})/j_{\text{Ocorr}}] \quad (1)$$

where j_{Ocorr} and j_{corr} are the corrosion current densities for uninhibited and inhibited solutions, respectively. All the recorded j_{corr} values are converted into the corrosion rate (v_{Tafel}) in $\mu\text{m y}^{-1}$ (Millimeter per year; the penetration rate of corro-

sion through a metal) using the expression (Balaji and Upadhyaya, 2009):

$$v_{\text{Tafel}} = 3280 \times j_{\text{corr}} \times (M/nd) \quad (2)$$

where M is the atomic weight of Fe (55.85 g), n the number of electrons transferred in the corrosion reaction ($n = 2$) and d the density of Fe (7.88 g cm^{−3}).

EFM measurements were performed with applying potential perturbation signal with amplitude of 10 mV with two sine waves of 2 and 5 Hz. The Intermodulation spectra contain current responses assigned for harmonical and intermodulation current peaks. The larger peaks were used to calculate the corrosion current density (j_{corr}), the Tafel slopes (β_c and β_a) and the causality factors CF2 & CF3 (Bosch et al., 2001; Abd El Rehim et al., 2006).

All Electrochemical experiments were carried out using Gamry PCI300/4 Potentiostat/Galvanostat/Zra analyzer, DC105 Corrosion software, EFM140 Electrochemical Frequency Modulation software and Echem Analyst 5.21 for results plotting, graphing, data fitting & calculating. A corroded sample, immersed for 24 h in 0.5 M HCl solution containing 10 mM Ser, was subjected to XPS analysis using a Leybold Heraeus spectrometer with a hemispherical energy analyzer, working with a Mg anode and the MgK α line.

3. Results and discussion

3.1. Corrosion rate monitoring

Corrosion measurement employs a variety of techniques to determine how corrosive the environment is and at what rate metal loss is being experienced. Corrosion measurement is the quantitative method by which the effectiveness of corrosion control and prevention techniques can be evaluated and provides the feedback to enable corrosion control and prevention methods to be optimized. In this study, polarization and EFM measurements were selected as electrochemical dc and ac techniques to monitor corrosion rate, *vide infra*:

3.1.1. Electrochemical measurements

3.1.1.1. Polarization measurements. The generation of polarization curves continues to be important in aqueous corrosion research. The current (I) needed to maintain the metal (working electrode (WE)) at each applied potential (E_w) is ascertained and the potential/current data is plotted to give the experimental polarization curve (Liening, 1986). In addition, polarization curves are useful in identifying the nature of the inhibition process. Thus, changes observed in the polarization curves after inhibitor addition are usually used as criteria to classify the inhibitor as cathodic, anodic or mixed (Cubley, 1990).

Fig. 2 presents Tafel polarization plots recorded for steel in aerated 0.50 M HCl solution without and with Ser of various concentrations (1.0–5.0 mM) at 30 °C. It is seen that the polarization curves display a well-defined cathodic Tafel region. However, the anodic polarization curve does not display an extensive Tafel region, may be due to passivation and pitting (see the inflection in the anodic branch). Corrosion currents and the other electrochemical kinetic parameters (Table 1) associated with polarization measurements were measured based on the method presented in our previous studies (Amin et al., 2009a; Amin et al., 2009b).

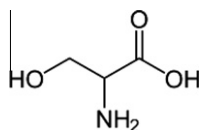


Figure 1 Chemical structure of serine molecule.

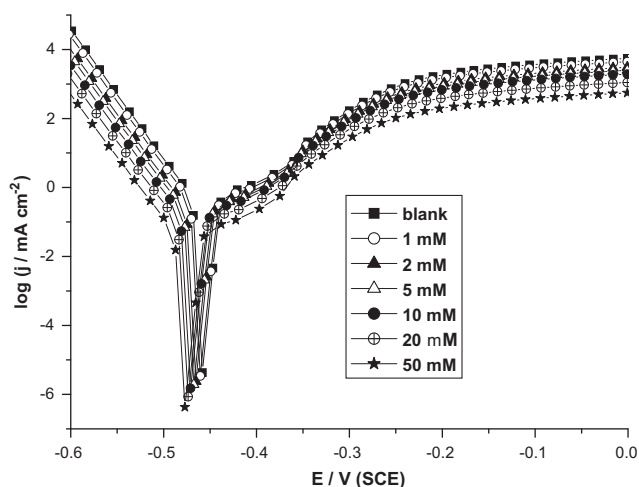


Figure 2 Polarization curves recorded for steel in aerated 0.50 M HCl solutions without and with various concentrations (1.0–50 mM) of Ser at a scan rate of 0.50 mVs⁻¹ at 30 °C.

As it can be seen, the corrosion potential (E_{corr}) shifts in the negative direction and both cathodic and anodic reactions of steel corrosion were inhibited with the increase of Ser concentration. In addition, values of j_{corr} decrease with increase in Ser concentration. This compound therefore exerted an efficient inhibitory effect both on anodic dissolution of the low alloy steel and on cathodic hydrogen evolution reaction. However, Ser suppressed the cathodic reaction to greater extents than the anodic one. Based on these results, Ser acts mainly as a cathodic-type inhibitor. It has been shown that the amino acids act as inhibitors through adsorption on the metal surface (His et al., 1990; Gommaa and Wahdanb, 1994). These amino acids can be protonated at the amine group in acidic solution, and can be adsorbed to cathodic sites of the electrode surface. Thus, they hinder the cathodic reaction and acts as cathodic inhibitors.

It is obvious that the shapes of the polarization plots for inhibited electrodes are not substantially different from those of uninhibited electrodes. The presence of Ser decreases the corrosion rate but does not change other aspects of the behaviour. This means that the inhibitor does not alter the electrochemical reactions responsible for corrosion. In addition, the absence of significant changes in the cathodic Tafel slope in the presence of inhibitor indicates that the hydrogen evolution

is slowed down by the surface blocking effect of the inhibitor. This indicates that the inhibitive action of Ser, may be related to its adsorption and formation of a barrier film on the electrode surface. XPS examinations of the electrode surface confirmed the existence of inhibitor adsorbed film; see more details in Section 3.2.

The effect of temperature on the inhibited acid-metal reaction is highly complex, because many changes occur on the metal surface, such as rapid etching and desorption of the inhibitor and the inhibitor itself, in some cases, may undergo decomposition and/or rearrangement. The effect of temperature on the cathodic and anodic polarization curves of steel in 0.50 M HCl solution without and with various concentrations of Ser was also studied (data not shown here). The obtained data showed that increasing the solution temperature, irrespective of the absence or presence of the inhibitor, leads to increasing the current density values of the two branches of the polarization curves and consequently the values of j_{corr} . Moreover, cathodic shifts were observed in the corrosion potential (E_{corr}) values at higher temperatures. This result reflects the enhancement of both the cathodic hydrogen evolution reaction and anodic corrosion reaction with temperature. Table 2, as an example, collects the various electrochemical parameters, together with the rates of corrosion and inhibition efficiency values, recorded for steel in 0.5 M HCl solution containing 10 mM Ser as a function of temperature. It follows from the data of Table 2 that the rate of corrosion enhances, while the inhibition efficiency values decrease with increase in temperature.

It is seen that Ser has inhibiting properties at all the studied temperatures and the values of $I(\%)$ decrease with temperature increase. This shows that the inhibitor has experienced a significant decrease in its protective properties with increase in temperature. This decrease in the protective properties of the inhibitor with increase in temperature may be connected with two effects; a certain drawing of the adsorption-desorption equilibrium towards desorption (meaning that the strength of adsorption process decreases at higher temperatures) and roughening of the metal surface which results from enhanced corrosion. These results suggest that physical adsorption may be the type of adsorption of the inhibitor on the steel surface.

3.1.1.2. Electrochemical frequency modulation method. Compared to chemical methods, electrochemical techniques can obtain the instantaneous corrosion rate, implement in-situ measurement, and provide plenty of information. Thus, they

Table 1 Electrochemical parameters, inhibition efficiencies ($I(\%)$) and corrosion rates (v) associated with Tafel polarization and EFM measurements, for steel in 0.5 M HCl solutions without and with various concentrations of Ser at 30 °C.

[Ser] (mM)	Tafel polarization				EFM				
	E_{corr} (mV (SCE))	j_{corr} (mA cm ⁻²)	β_a (mV dec ⁻¹)	$-\beta_c$ (mV dec ⁻¹)	v_{Tafel} (μ^{-1})	I_{Tafel} (%)	v_{EFM} (μ^{-1})	I_{EFM} (%)	j_{corr} (mA cm ⁻²)
Blank	-459	0.2	86	55	2.32	–	2.56	–	0.22
1	-461	0.16	88	54	1.86	19.25	1.98	21	0.17
2	-465	0.11	87	56	1.28	45.73	1.39	43.88	0.12
5	-468	0.09	85	55	1.05	55	1.16	58	0.10
10	-471	0.07	87	55	0.81	67	0.70	69.54	0.06
20	-475	0.04	86	57	0.46	82	0.41	83.88	0.035
50	-478	0.02	85	58	0.23	91	0.17	93.05	0.015

Table 2 Electrochemical parameters, inhibition efficiencies ($I(\%)$) and corrosion rates (v) associated with Tafel polarization and EFM measurements, for steel in 0.5 M HCl solution containing 10 mM Ser at different temperatures.

T (K)	Tafel polarization				EFM				
	E_{corr} (mV (SCE))	j_{corr} (mA cm ⁻²)	β_a (mV dec ⁻¹)	$-\beta_c$ (mV dec ⁻¹)	v_{Tafel} (μ^{-1})	I_{Tafel} (%)	v_{EFM} (μ^{-1})	I_{EFM} (%)	j_{corr} (mA cm ⁻²)
283	-454	0.02	87	57	0.23	82	0.21	81	0.018
293	-465	0.05	86	55	0.58	75	0.55	76	0.047
303	-471	0.07	87	55	0.81	67	0.70	69.54	0.06
313	-477	0.12	91	65	1.39	61	1.28	60	0.11
323	-482	0.22	102	78	2.56	52	2.79	53	0.24
333	-495	0.43	118	91	5.00	38	4.77	41	0.41

are expected to be applied to detect and monitor corrosion of metals and alloys in various corrosive media. Several electrochemical techniques are available to determine corrosion rate, such as the linear polarization resistance (LPR) technique, Tafel-extrapolation, and electrochemical impedance spectroscopy (EIS).

The LPR and EIS techniques require B value to calculate corrosion rate from polarization resistance R_p according to the equation $j_{\text{corr}} = B/R_p$. And Tafel-extrapolation measurement, despite of its application here to evaluate corrosion rates, is time consuming and will damage the electrode surface due to the polarization over a wide potential range. Compared with these three electrochemical techniques, EFM technique can quickly determine the corrosion current value without prior knowledge of Tafel slopes, and with only a small polarizing signal. These advantages of EFM technique make it an ideal candidate for online corrosion monitoring (Kus and Mansfeld, 2006).

The main objective of performing EFM measurements is to confirm validation of corrosion rates measured by Tafel extrapolation method, one of the most popular DC techniques for estimation of corrosion rate. The EFM intermodulation spectra (spectra of current response as a function of frequency) of steel in 0.50 M HCl solutions devoid of and containing various concentrations of Ser have been studied (data not presented here). The values of causality factors obtained under different experimental conditions were approximately equal the theoretical values (two and three) indicating that the measured data are of quality (Gommaa and Wahdanb, 1994).

Corrosion currents, $(j_{\text{corr}})_{\text{EFM}}$, were calculated as a function of Ser concentration (see also Table 1) using equations presented elsewhere (Rehim et al., 2008). These $(j_{\text{corr}})_{\text{EFM}}$ values were inserted in Eqs. (1) and (2) to calculate inhibition efficiency $I_{\text{EFM}}(\%)$ and corrosion rates (v_{EFM}), respectively. The recorded values of $I_{\text{EFM}}(\%)$ and v_{EFM} were also collected in Table 1. Addition of increasing concentrations of Ser to HCl solution decreases the corrosion current density, indicating that Ser inhibits the corrosion of steel through adsorption. The calculated inhibition efficiency enhances with Ser concentration. It is quite obvious that the data obtained from Tafel extrapolation method were in a good agreement with the results obtained from the EFM technique.

The EFM parameters have also been calculated at different temperatures and listed in Table 2. Inspection of the data of Table 2 reveals that the temperature increase leads to an essential decrease of the inhibition efficiency ($I_{\text{EFM}}(\%)$) values which on one hand may be attributed to the corrosion rate increase and on the other hand to the probable partial

desorption of the inhibitor under these conditions. However, it seems that an inhibiting adsorption layer exists at any given temperature. It may be assumed that the density of the inhibitor adsorbed layer within outer Helmholtz layer (OHL) decreases, while the diffuse part of the double electrical layer increases with temperature. This effect is accompanied by a certain increase in the rate of corrosion and surface roughness. It is apparent that the inhibition efficiency increases with increasing inhibitor concentration, while it decreases with increasing temperature, confirming the suggestion that physical adsorption occurs. It is worth noting from Tables 1 and 2 that the rates of corrosion and the inhibition efficiencies obtained from the EFM method are comparable and run parallel with those obtained from the Tafel extrapolation method. These findings confirm corrosion rates measured by the Tafel extrapolation method.

3.2. XPS examinations

The formation of a protective surface film of inhibitor at the electrode surface was further confirmed by XPS examinations of the electrode surface. Fig. 3 presents the XPS recorded for steel immersed in 0.5 M HCl solution containing 10 mM Ser for 24 h at E_{corr} . XPS spectra of the N(1s) confirmed the protonation of nitrogen in the Ser molecule. The N(1s) spectra

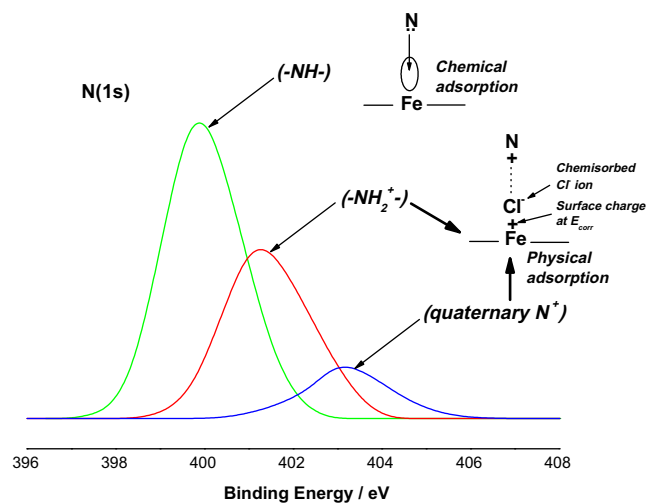


Figure 3 The N(1s) photoelectron spectra recorded for steel immersed for 12 h in 0.5 M HCl solution containing 10 mM Ser at E_{corr} at 30 °C.

presented in Fig. 3 can be deconvoluted into component bands at 399.9 ± 0.2 eV ($-\text{NH}-$), 401 ± 0.2 eV ($-\text{NH}_2^+$) and 402.9 ± 0.2 eV (quaternary N^+), respectively. Two chemically distinct adsorbed Ser species were detected in the experiment, namely 399.9 eV for the unprotonated N ($\text{N}:$), and 401.3 eV and 402.8 eV for the protonated NNH_2^+ and quaternary N^+ .

Two possible mechanisms of Ser adsorption can be presented see the different modes of adsorption in the insert of Fig. 3. The first may be direct physisorption (electrostatic in nature) of protonated Ser species on the electrode surface already charged with a negative layer of chemisorbed Cl^- ions (Rehim et al., 2008). The second may be chemical adsorption owing to the coordinate bonds formed between the lone electron pairs of the unprotonated N-atoms and the empty orbits of Fe atoms.

3.3. Adsorption isotherms and standard free energy of the adsorption process

The steel corrosion inhibition by Ser can be explained by its adsorption so as to impede the adsorption of the aggressive species in the corrosive solution. The adsorption on the corroding surfaces never reaches the real equilibrium and tends to reach an adsorption steady state. However, when the corrosion rate is sufficiently small, the adsorption steady state has a tendency to become a quasi-equilibrium state. In this case, it is reasonable to consider the quasi-equilibrium adsorption in thermodynamic way using the appropriate equilibrium adsorption isotherms (Vracar and Drazic, 2002).

The extent of corrosion inhibition depends on the surface conditions and the mode of adsorption of the inhibitors (Khairou and El-Sayed, 2003). Under the assumptions that the corrosion of the covered parts of the surface is equal to zero and that corrosion takes place only on the uncovered parts of the surface (i.e., inhibitor efficiency is due mainly to the blocking effect of the adsorbed species), the degree of surface coverage (θ) has been estimated from the chemical and electrochemical techniques employed in this study as follows: $\theta = I(\%)/100$ (assuming a direct relationship between surface coverage and inhibition efficiency) (Moretti et al., 1996; de Damborenea and Bastidas, 1997; Christov and Popova, 2004; Bentiss et al., 1999).

The values of surface coverage to different concentrations of inhibitors, obtained from the Tafel extrapolation and the EFM measurements at different temperatures, have been used to explain the best isotherm to determine the adsorption process. Adsorption isotherms are very important in determining the mechanism of organo-electrochemical reactions (Khairou and El-Sayed, 2003). The most frequently used isotherms are Langmuir, Hill de Boer, Parsons, Temkin, Flory-Huggins and Dahar-Flory-Huggins and Bockris-Swinkell (Moretti et al., 1996; de Damborenea and Bastidas, 1997; Christov and Popova, 2004; Bentiss et al., 1999; Damaskin, 1971; Langmuir and Am, 1917; Alberty and Silbey, 1997). All these isotherms are of the general form:

$$f(\theta, x) \exp(2a\theta) = KC \quad (3)$$

where $f(\theta, x)$ is the configurational factor which depends upon the physical model and the assumptions underlying the derivation of the isotherm, θ the surface coverage degree, C the inhibitor concentration in the bulk of solution, “ a ” the lateral

interaction term describing the molecular interactions in the adsorption layer and the heterogeneity of the surface and is a measure for the steepness of the adsorption isotherm. K is the adsorption–desorption equilibrium constant.

In the range of temperature studied (283–333 K), The best correlation between the experimental results, obtained from the two techniques, and the isotherm functions was obtained using Temkin adsorption isotherm (Eq. (4)).

$$\exp(2a\theta) = KC \quad (4)$$

Fig. 4, as a representative example, shows fitting of the Tafel extrapolation and EFM data obtained for steel electrode in 0.50 M HCl solutions containing various concentrations of Ser to Temkin isotherm at 303 K. Similar plots were obtained for the other tested temperatures. The values of correlation coefficient (R^2) were used to determine the best fit isotherm. Perfectly linear plots were obtained with correlation coefficient of (0.997 and 0.998). The isotherms’ parameters (K and a) and the free energies of the inhibitor adsorption (ΔG_{ads}^0) calculated from the equation (O’M. Bockris and Khan, 1993):

$$K = (1/55.5) \exp(\Delta G_{\text{ads}}^0 / RT) \quad (5)$$

are shown in Table 3 as a function of temperature. The number 55.5 refers to the concentration of water in the solution in mol l^{-1} , R the universal gas constant, T the thermodynamic temperature.

It follows from the data of Table 3 that the values of K are relatively high and decrease with temperature. It is well-known that large values of K mean better inhibition efficiency of the inhibitor, i.e., strong electrical interaction between the double layer existing at the phase boundary and the adsorbing inhibitor molecules. On the other hand, small values of K , however, compromise such interactions between adsorbing inhibitor molecules and the metal surface so that the inhibitor molecules are easily removable by the solvent molecules from the surface. These results confirm the suggestion that this inhibitor is physically adsorbed and the strength of adsorption decreases with temperature. Positive values of “ a ” may indicate the existence

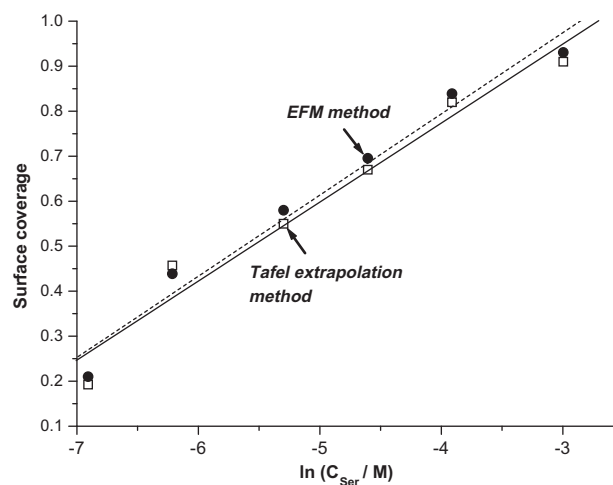


Figure 4 Fitting of the surface coverage, derived from Tafel extrapolation and EFM techniques, for steel in 0.50 M HCl solution containing various concentrations of Ser to Temkin adsorption isotherm at 303 K.

Table 3 Adsorption parameters (K and a) and the free energy of adsorption (ΔG_{ads}^0) recorded for steel in 0.5 M HCl solution containing 10 mM Ser. Data obtained from the Tafel extrapolation and the EFM methods after fitting the results with the Temkin isotherm at different temperatures.

T (K)	Tafel polarization			EFM		
	K	a	$-\Delta G_{\text{ads}}^0$ (kJ mol $^{-1}$)	K	a	$-\Delta G_{\text{ads}}^0$ (kJ mol $^{-1}$)
283	27500	3.22	33.44	26982	3.05	33.40
293	11250	2.98	32.45	10995	2.83	32.40
303	4469	2.85	31.24	4448	2.77	31.25
313	2237	2.22	30.47	2120	2.18	30.33
323	1050	1.95	29.42	866	1.91	28.90
333	320	1.87	27.04	288	1.82	26.75

of lateral forces of attraction between adsorbate molecules in the adsorption layer (O'M. Bockris and Khan, 1993).

The negative value of ΔG_{ads}^0 ensures the spontaneity of the adsorption process and stability of the adsorbed layer on the electrode surface. This stability of the adsorbed layer decreases with increase in temperature. This is clearly seen from the decrease in the absolute value of ΔG_{ads}^0 with the rise in temperature (see again Table 3). This also favours physical adsorption. Generally, values of ΔG_{ads}^0 lower than -40 kJ mol $^{-1}$ are consistent with the electrostatic interaction between the charged molecules and the charged metal (physi-sorption); those around -50 kJ mol $^{-1}$ or higher involve charge sharing or charge transfer from organic molecules to the metal surface to form a coordinate type of bond (chemi-sorption) Albery and Silbey, 1997; Schapinik et al., 1960.

Based on the data presented in Table 3, the calculated value of ΔG_{ads}^0 , obtained from the two methods employed, was found to be lower than -40 kJ mol $^{-1}$. This confirms the occurrence of physical adsorption. Thus, the most probable mechanism of Ser adsorption is the physical type; inspect again modes of adsorption presented in the insert of the XPS spectra (Fig. 3). In general, the proceeding of physical adsorption requires the presence of both electrically charged metal surface and charged species in the bulk of the solution.

3.4. Apparent activation energy of the corrosion process

The temperature increases the rate of all electrochemical processes and influences adsorption equilibria and kinetics as well. Temperature investigations allow the determination of activation energy, pre-exponential factor and other thermodynamic activation functions in absence and in presence of inhibitor. The obtained results can elucidate the mechanism of corrosion inhibition. In the present work, further insight into the adsorption mechanism is offered by considering the apparent activation energies (E_a^o) for the steel dissolution in HCl solutions in the absence and presence of different concentrations of the tested inhibitor. The apparent activation energies were obtained by applying the well-known Arrhenius Equation (O'M. Bockris and Reddy, 1977):

$$\ln(\text{rate}) = -(E_a^o/RT) + \ln A \quad (6)$$

Arrhenius plots obtained from the Tafel extrapolation and EFM methods were constructed for steel in 0.50 M HCl solutions containing various concentrations of Ser in the range of temperature (283–333 K). Fig. 5 represents the Arrhenius plots, obtained from the two methods, of steel in 0.50 M

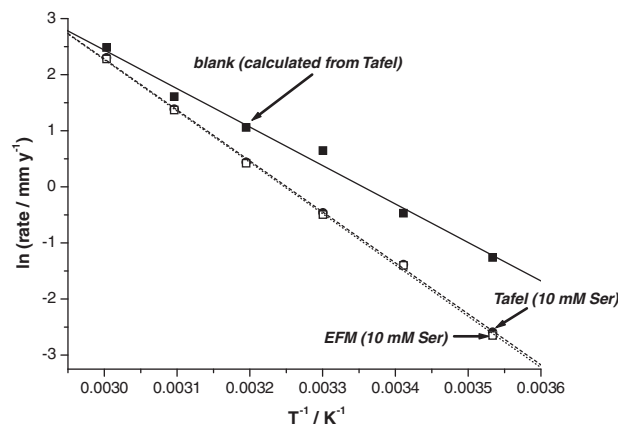


Figure 5 Arrhenius plot of the corrosion rate, obtained from the Tafel extrapolation and EFM methods, recorded for steel in 0.50 M HCl without and with 10 mM Ser.

HCl solution containing 10 mM Ser (as an example). Similar trend was obtained for the other tested concentrations of the inhibitor. The values of E_a^o were calculated from these plots and listed in Table 4 as a function of Ser concentration. The value of 57 kJ mol $^{-1}$ obtained for the activation energy E_a^o of the corrosion process in 1.0 M HCl lies in the range of the most frequently cited values, the majority of which are grouped around 60.7 kJ mol $^{-1}$ (Riggs and Hurd, 1967). The higher values of E_a^o in presence of the inhibitor than in its absence can be interpreted as an indication of physical adsorption.

Table 4 Values of the apparent activation energies (E_a^o) recorded for steel in 0.5 M HCl solutions without and with various concentrations of Ser. Data obtained from the Tafel extrapolation and the EFM methods after applying Arrhenius equation.

[Ser] (mM)	E_a^o (kJ mol $^{-1}$)	
	Tafel extrapolation method	EFM method
Blank	56.91	57.22
1	62.88	63.12
2	65.91	66.41
5	71.00	71.21
10	75.45	75.90
20	82.54	83.00
50	92.05	91.55

The increase in E_a^o is proportional to the inhibitor concentration, indicating that the energy barrier for the corrosion interaction is also increased (Szauer and Brandt, 1981; El Sherbini, 1999; Bastidas et al., 1997). This means that the corrosion reaction will be further pushed to the surface sights that are characterised by progressively higher values of E_a^o as the concentration of the inhibitor in the solution becomes larger. In other words, the adsorption of the inhibitor on the electrode surface leads to the formation of a physical barrier that reduces the metal reactivity in the electrochemical reactions of corrosion (Mansfeld, 1987).

4. Conclusion

In this work, Tafel extrapolation method and EFM technique were employed to monitor corrosion rates of low alloy ASTM A213 grade T22 boiler steel in 0.5 M HCl solutions without and with various concentrations of serine (Ser) as a safe-inhibitor. The principle conclusions are:

- (i) Ser exhibited good inhibiting properties for low alloy steel corrosion in 0.50 M HCl solutions.
- (ii) The inhibition efficiency increases with the increase in Ser concentration, while it decreases with temperature, suggesting the occurrence of physical adsorption.
- (iii) Tafel polarization plots of Ser indicated that this compound acts mainly as a cathodic-type inhibitor.
- (iv) Rates of corrosion and inhibition efficiencies obtained from Tafel extrapolation method and EFM technique were in good agreement.
- (v) XPS examinations of the steel surface confirm the existence of a protective adsorbed film of the inhibitor on the low alloy steel surface.
- (vi) Adsorption of Ser was found to follow Temkin isotherm.
- (vii) The investigated inhibitor was suggested to be physisorbed on the electrode surface on the basis of the low values of the free energy of adsorption (ΔG_{ads}^o : 26–33 kJ mol⁻¹).
- (viii) Apparent activation energies in the presence of Ser are higher than that in bare HCl solution. This is also referred by many researchers to physical adsorption.

References

- Abd El Rehim, S.S., Khaled, K.F., Abd-Elshafi, N.S., 2006. *Electrochim. Acta* 51, 3269.
- Alberty, R., Silbey R., *Physical Chemistry*, second ed., Wiley, New York, 1997, p. 845.
- Amin, M.A., Abd El Rehim, S.S., El-Naggar, M.M., Abdel-Fatah, H.T.M., 2009a. *J. Mater. Sci.* 44, 6258.
- Amin, M.A., Abd El Rehim, S.S., Abdel-Fatah, H.T.M., 2009b. *Corros. Sci.* 51, 882.
- Balaji, S., Upadhyaya, A., 2009. *J. Mater. Sci.* 44, 2310. doi:10.1007/s10853-008-3020-4.
- Bastidas, J.M., De Dambornea, J., Vazquez, A.J., 1997. *J. Appl. Electrochem.* 27, 345.
- Behpour, M., Ghoreishi, S.M., Gandomi-Niasar, A., 2009. *J. Mater. Sci.* 44, 2444. doi:10.1007/s10853-009-3309-7.
- Bentiss, F., Traisnel, M., Gengembre, L., Lagrenee, M., 1999. *Appl. Surf. Sci.* 152, 237–249.
- Bockris, J. O'M., Reddy, A.K.N. *Modern Electrochemistry*. vol. 2, Plenum Press, New York, 1977, p. 1267.
- Bockris, J. O'M., Khan, S.U.M., *Surface Electrochemistry: A Molecular Level Approach*, Plenum Press, New York, 1993.
- Bosch, R.W., Hubrecht, J., Bogaerts, W.F., Syrett, B.C., 2001. *Corrosion* 57, 60.
- Christov, M., Popova, A., 2004. *Corros. Sci.* 46, 1613–1620.
- Cubley, B.G. (Ed.), *Chemical Inhibitors for Corrosion Control*. The Royal Society of Chemistry, 1990.
- Damaskin, B.B., Petrii, O.A., Batrakov, B. *Adsorption of Organic Compounds on Electrodes*. Plenum Press, New York, 1971.
- de Dambornea, J., Bastidas, J.M., Vázquez, A.J., 1997. *Electrochim. Acta* 42, 455–459.
- El Sherbini, E.F., 1999. *Mat. Chem. Phys.* 60, 286.
- Gommaa, G.K., Wahdanb, M.H., 1994. *Mater Chem and Phys* 39, 142.
- His, A., Liedberg, B., Uvdal, K., Törnkvist, C., Bodjand, P., Lundstrom, I., 1990. *J. Colloid Interf. Sci.* 140, 192.
- Khairou, K.S., El-Sayed, A., 2003. *J. Appl. Polym. Sci.* 88, 866–871.
- Kus, E., Mansfeld, F., 2006. *Corros. Sci.* 48, 965.
- Langmuir, I., 1917. *J. Am. Chem. Soc.* 39, 1848–1906.
- Lebrini, M., Traisnel, M., Lagrenee, M., Mernari, B., Bentiss, F., 2008. *Corros. Sci.* 50, 473.
- Liening, E.L. In: Moniz, B.J., Pollock, W.I. (Eds.), *Process Industries Corrosion*, NACE, 1986, p. 85.
- Mansfeld, F., *Corrosion Mechanism*. Marcel Dekkar, New York, 1987 p. 119.
- Moretti, G., Quartarone, G., Trassan, A., Zingales, A., 1996. *Electrochim. Acta* 41, 1971–1980.
- Oguzie, E.E., Li, Y., Wang, F.H., 2007. *J. Colloid Interf. Sci.* 310, 90.
- Okayasu, M., Sato, K., Okada, K., et al., 2009. *J. Mater. Sci.* 44, 306. doi:10.1007/s10853-008-3053-8.
- Rao, V.S., Singhal, L.K., 2009. *J. Mater. Sci.* 44, 2327. doi:10.1007/s10853-008-2976-4.
- Rehim, Abd.El., Hazzazi, O.A., Amin, M.A., Khaled, K.F., 2008. *Corros. Sci.* 50, 2258.
- Riggs, O.L., Hurd, R.M., 1967. *Corrosion* 23, 252.
- Schapinik, J.W., Oudeman, M., Leu, K.W., Helle, J.N., 1960. *Trans. Farad. Soc.* 56, 415–423.
- Sundararajan, G., Phani, P.S., Jyothirmayi, A., 2009. *J. Mater. Sci.* 44, 2320. doi:10.1007/s10853-008-3200-2.
- Szauer, T., Brandt, A., 1981. *Electrochim. Acta* 26, 943.
- Vracar, Lj., Drazic, D.M., 2002. *Corros. Sci.* 44, 1669–1689.